

## Short Communication

Solar flare impact on FUV based thermospheric O/N<sub>2</sub> estimation

Y. Zhang\*, L.J. Paxton, H. Kil

The Johns Hopkins University Applied Physics Laboratory, Laurel, USA

## ARTICLE INFO

## Article history:

Received 2 June 2016

Received in revised form

27 June 2016

Accepted 28 June 2016

Available online 29 June 2016

## Keywords:

Thermospheric composition

Solar flare

## ABSTRACT

During/after intense solar flares, FUV based thermospheric O/N<sub>2</sub> ratio decreases and recovers instantly, indicating that the decrease is not physical. Simulations with an increased solar X-ray (0–10 nm) flux and a fixed O and N<sub>2</sub> profiles show a significant 135.6 nm/LBHS decrease that is sufficient to explain the O/N<sub>2</sub> decrease. The false O/N<sub>2</sub> decrease is mostly due to increased differences in O<sub>2</sub> absorption at 135.6 nm and LBHS caused by low-altitude emissions associated with enhanced X-rays. However, the heating from solar flares may cause a weak depletion in O/N<sub>2</sub>.

© 2016 Elsevier Ltd. All rights reserved.

## 1. Introduction

Solar flares are the sudden enhancements in solar radiation across a wide wavelength range, especially in the EUV and X-ray bands that impact the thermosphere and ionosphere significantly. A number of studies revealed that the thermospheric density, temperature and ionospheric density increases during solar flares (Sutton et al., 2006; Liu et al., 2007; Pawlowski and Ridley, 2008, 2011; Qian et al., 2011; Le et al., 2012; Zhu and Ridley, 2014). The two intense X17 flares on October 28 and November 4, 2003 attracted lots of attention. Using the CHAMP and GRACE neutral density measurements at altitude ~400 and 490 km, Sutton et al. (2006) found the thermospheric density increased by 50–60% at low and mid-latitudes associated with the October 28 flare. The enhanced density took about 12 h to return to pre-flare values. The flare on November 4, 2003 led to a density increase of ~35 to 45% with a similar recovery time. The density enhancements indicate an exosphere temperature increase of about 125–175 K and 100–125 K, respectively. The neutral density from the CHAMP satellite also showed a rapid (in a few minutes) response to the October 28, 2003 flare and a 20% increase almost homogeneously at all latitudes below 50°N/S (Liu et al., 2007). Using the Global Ionosphere and Thermosphere (GITM) model, Pawlowski and Ridley (2008) found that the modeled neutral density increased rapidly (up to ~15%) at 400 km within 2 h of the October 28 and November 4, 2003 flares. The GITM output also revealed the creation of gravity waves after the flares. Furthermore, GITM simulations show divergent horizontal wind around the sub-solar point and convergent wind on the nightside. Qian et al. (2011) did simulations

for weaker flares (X6.2 and X5.4) and they found that the neutral density at CHAMP altitude was enhanced by ~15 to 20% and ~5%, respectively. A statistical analysis of the solar flares between 2001 and 2006 indicates that the neutral density at the CHAMP altitudes increased 10–13% on average for X5 and stronger flares (Le et al., 2012).

These earlier studies (and references therein) significantly advanced our understanding of the thermospheric response to solar flares. However, these studies focused on neutral density and temperature around the 400–500 km where in situ satellite measurements are available. What is the response of lower thermosphere (100–200 km)? TIMED/GUVI based O/N<sub>2</sub> shows significant decrease during intense solar flares. Is the O/N<sub>2</sub> decrease real? In this paper, we report the impact of solar flares in estimating the O/N<sub>2</sub> ratios.

## 2. TIMED/SEE solar flux data

The Solar EUV Experiment (SEE) instrument on the NASA TIMED satellite measures the solar spectral irradiances from 0.1 to 194 nm in 1 nm intervals (Woods et al., 2005). Fig. 1 shows the total flux in the wavelengths between 0 and 105 nm. The solar flux data are obtained from the NASA space physics database at <http://cdaweb.gsfc.nasa.gov/>. Most contribution to the total flux comes from irradiance between 0 and 7 nm. Three major flares are marked by black arrows with date and UT. There are two or more minor flares during the period. The Dst index is also plotted (red line) in Fig. 1. It is clear that the major flares occurred before a major geomagnetic storm, after recovery from the storm, and during a recovery from a minor geomagnetic storm, respectively. These intense flares provide an opportunity to examine the

\* Corresponding author.

E-mail address: [yongliang.zhang@jhuapl.edu](mailto:yongliang.zhang@jhuapl.edu) (Y. Zhang).

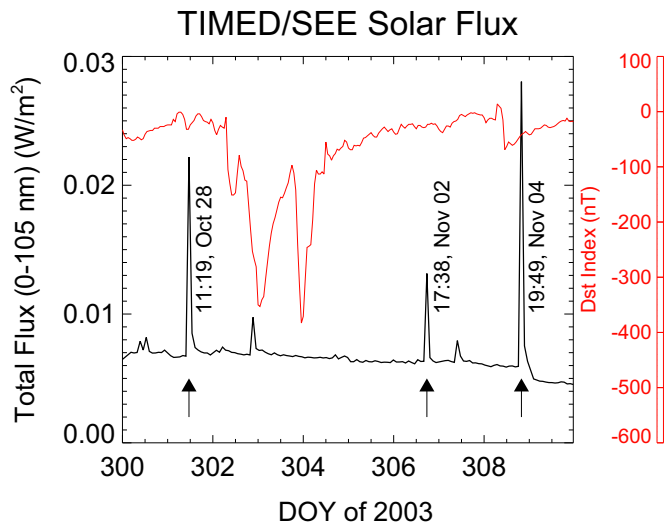


**Fig. 1.** Total flux (black line) of solar EUV and X-ray (0–105 nm) from TIMED/SEE between DOY 300 (October 27) and 309 (November 5), 2003. There are three major flares marked by black arrows. The red line is for Dst index. (For interpretation of the references to color in this figure legend, the reader is referred to the web version of this article.)

thermospheric  $O/N_2$  response without contamination from the storm-time  $O/N_2$  changes or depletions (Zhang et al., 2004).

### 3. TIMED/GUVI $O/N_2$ data

The Global Ultraviolet Imager (GUVI) on NASA TIMED satellite provides cross-track scanned images of the Earth's airglow and auroral emission in the far ultraviolet (FUV) at wavelengths  $\sim 110.0$  to  $185.0$  nm (Paxton and Meng, 1999; Christensen et al., 2003; Paxton et al., 2004). Major emission features include HI (Lyman  $\alpha$ , 121.6 nm), OI (130.4 nm), and OI (135.6 nm) lines; and  $N_2$  LBHS (140.0–150.0 nm) and  $N_2$  LBHL (165.0–180.0 nm) bands. The dayglow data in the 135.6 nm and LBHS bands (135.6 nm/LBHS intensity ratios) have been used to estimate the thermospheric  $O/N_2$  column density ratios (Zhang et al., 2004). Fig. 2a, the GUVI  $O/N_2$  map on October 28, 2003, shows typical geomagnetic quiet time  $O/N_2$  distributions: relatively smooth  $O/N_2$  and a south–north gradient due to the seasonal effect (low  $O/N_2$  in summer hemisphere) and localized  $O/N_2$  depletion in the northern high latitude and the southern region around Australia (due to a large shift of the southern geomagnetic pole from the southern geographic pole). However, there is a narrow longitude region in the Indian Ocean sector where the  $O/N_2$  shows an anomaly: latitude independent depletion (marked by a red arrow). The  $O/N_2$  over a wide latitude region ( $\sim -50^\circ$  to  $50^\circ$ ) is significantly lower than the values over Asia or Africa sectors. Note that the  $O/N_2$  map consists of GUVI data over 14 orbits for a given day at roughly a fixed local time ( $\sim 16:00$ LT). This means that the  $O/N_2$  pixels in the map have different UT. The UT and local time (LT) of the pixels with smallest solar zenith angle (SZA) for one of every two orbits are marked at the bottom of the  $O/N_2$  map. The UT increases from right to left as Earth rotates under the TIMED orbit at a roughly fixed LT over a few days. The  $O/N_2$  anomaly (depletion) was observed over a single orbit. The undisturbed  $O/N_2$  in the Asia and Africa sectors was observed before and after the  $O/N_2$  anomaly (roughly 3 h difference as TIMED orbit period is  $\sim 1.5$  h). The  $O/N_2$  anomaly occurred during geomagnetic quiet time. This is different from the geomagnetic storm-time  $O/N_2$  depletion that extends from high to mid and low latitudes (Zhang et al., 2004, 2014). The storm-time  $O/N_2$  depletion does not penetrate through the equatorial region

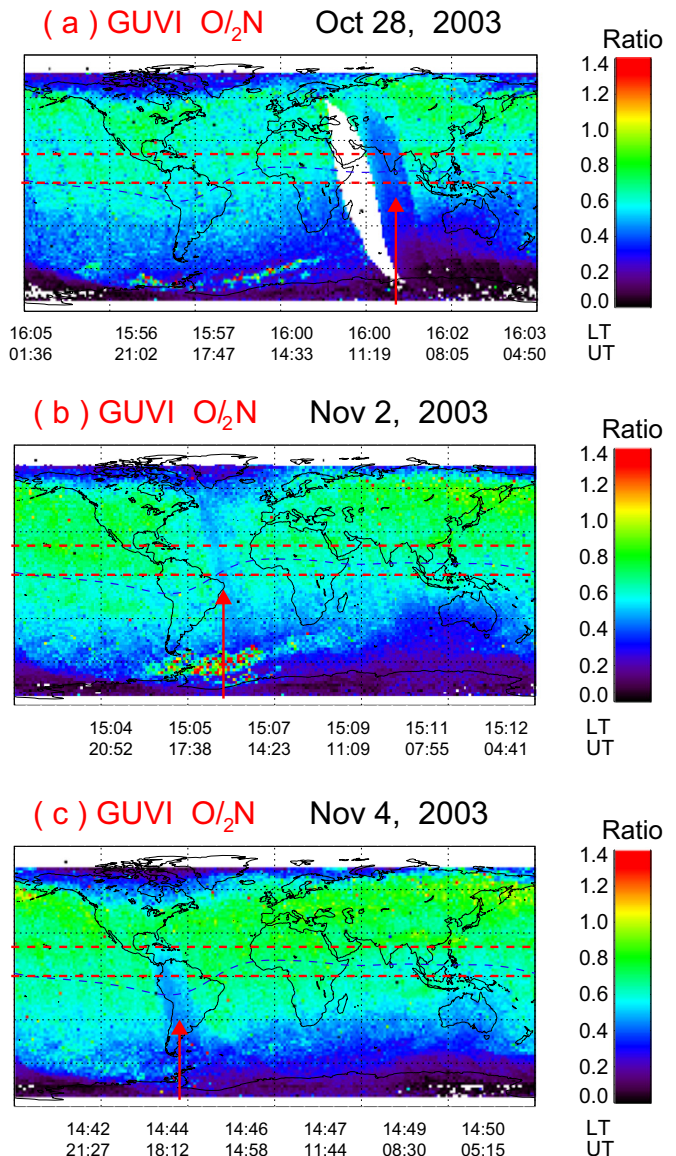


**Fig. 2.** TIMED/GUVI  $O/N_2$  maps on October 28, November 2 and November 4, 2003. The red arrows indicate the time when the  $O/N_2$  depletion anomalies were observed. (For interpretation of the references to color in this figure legend, the reader is referred to the web version of this article.)

with a depletion tunnel connecting  $O/N_2$  depletion regions in both hemispheres. What causes this  $O/N_2$  depletion anomaly under geomagnetic quiet conditions? Similar  $O/N_2$  anomalies were also obtained on November 2 and 4, 2003 (see Fig. 2b,c as marked by red arrows).

The above three  $O/N_2$  anomalies (Fig. 2) were associated with intense solar flares seen in Fig. 1. To examine the details, the GUVI  $O/N_2$  values between latitudes  $0^\circ$  and  $20^\circ$  are averaged for each GUVI orbit to get mean  $O/N_2$ . Statistical deviations (or errors) from the means are calculated. The mean UT of the  $O/N_2$  pixels is also obtained. Fig. 3a is similar to Fig. 1 but for a shorter period of time (DOY 300–303) with the mean  $O/N_2$  and deviations/errors (blue color) plotted. The statistical errors are about 10% of the mean  $O/N_2$  and represent the background uncertainties. The black arrow in Fig. 3a indicates the time (11:19 UT, October 28, 2003) when the flare peaked. Interestingly, the mean  $O/N_2$  (blue diamond) shows a clear drop of  $\sim 27\%$  (from  $\sim 0.60$  to  $\sim 0.44$ ). The 27% drop is bigger than the statistical error or background variation ( $\sim 10\%$ ) so it is significant. The associated peak solar flux is  $0.022$   $W/m^2$ .

Download English Version:

<https://daneshyari.com/en/article/1776173>

Download Persian Version:

<https://daneshyari.com/article/1776173>

[Daneshyari.com](https://daneshyari.com)